Minimization of Exergy Losses in the COREX Process

AMEYA KADROLKAR, S.K. ROY, and P.K. SEN

The COREX process is being projected as an alternative for blast furnace iron making. The coal consumption of the COREX process is large with a net fuel rate of ~1000 kg/tone of hot metal (THM). The reason for a higher net fuel rate of the COREX process compared with the net coal rate for the blast furnace process has been investigated. Exergy analysis has been performed for identifying the causes, locations, and magnitudes of process inefficiencies for the COREX process. Whereas blast furnace process data are available in the literature, no systematic data for stream information of the COREX process are available for different input coal rates required for exergy computation. A composite model of the COREX process (*i.e.*, models for the smelter gasifier and the reduction shaft) using FactSage 6.2 (Thermfact/CRCT, Montreal, Canada, and GTT Technologies, Aachen, Germany) is used to generate stream data. A new methodology for the calculation of exergy of the COREX process streams using the database in FactSage is proposed in this work. Exergy data for blast furnace process streams have been obtained from the literature. The exergy loss and exergy efficiencies of the COREX process are evaluated at various coal rates and compared with those of the blast furnace. Operating the COREX process is theoretically feasible at lower coal rates with higher exergy efficiencies when lesser export gas is generated.

I. INTRODUCTION

THE COREX process is being projected as an alternative for blast furnace iron making, which is heavily dependent on coke because good quality coking coal is becoming a scarce commodity. The coal consumption in the COREX process is comparatively large with a fuel rate (noncoking coal and coke) of ~1000 kg/tone of hot metal (THM) as has been estimated by Prachethan Kumar *et al.*[1] This gives rise to the question of its viability compared with blast furnace regarding optimal resource use. Exergy analysis helps in identifying the causes, locations, and magnitudes of inefficiencies of a process, and it provides better insights on the means to improve the process performance. An exergy analysis is more effective than energy analysis because it takes into account the limitations imposed on a process by the second law of thermodynamics. deBeer *et al.*[2] attempted to compare the performance of the COREX process with other iron making processes (like blast furnace) and the different smelting-reduction processes with respect to their specific energy consumptions and production cost of hot metal. Costa *et al.*[3] compared exergy losses and efficiencies of integrated steelworks incorporating COREX as well as conventional blast furnace processes. However, there is no report as yet where the COREX process has been examined through rigorous exergy analysis even though, previously, some other iron-making processes have been

analyzed through exergy analysis. Exergy consumption of blast furnace for a range of operating conditions has been predicted through exergy and energy consumption indices by Petela *et al.*[4] Ostrovski and Zhang[5] compared the exergy loss in the blast furnace and direct iron ore smelting process, whereas Nogami *et al.*[6] compared the performances of conventional and charcoal-charged blast furnaces through exergy analyses. However, in these reports, the exact methodology adopted for exergy calculation of streams is not mentioned properly.

A detailed exergy analysis of the COREX process and its comparison with analyses of other iron-making processes would provide useful insights into optimal resource utilization. Furthermore, such an analysis can reveal whether there is a scope for optimization of resource consumption through the production of other useful outputs such as power.

A methodology for the exergy calculation of metallurgical process streams like hot metal and slag (while considering detailed phase composition) is proposed in this work. Based on the results of this analysis, exergy efficiencies were predicted and compared with those for the blast furnace obtained from the literature.

In Section II, the thermodynamic models for the smelter gasifier as well as the reduction shaft are proposed and their validations are discussed. In Section III, the methodology for the exergy calculation of compounds and mass streams is outlined through the use of thermodynamic calculation software, FactSage (Thermfact/CRCT, Montreal, Canada, and GTT Technologies, Aachen, Germany). The methodology is validated by comparison with the published literature data. In Section IV, the methodology is applied to the COREX process, and a detailed exergy analysis is presented under its various operating conditions. Furthermore,

AMEYA KADROLKAR, Graduate Student, and S.K. ROY and P.K. SEN, Professors, are with the Department of Metallurgical and Materials Engineering, Indian Institute of Technology, Kharagpur 721302, India. Contact e-mail: pksen@metal.iitkgp.ernet.in

exergy efficiencies of the process at various input coal rates are predicted and compared with the published data on blast furnace. Section V presents a summary and conclusions drawn from the work.

II. DEVELOPMENT OF THERMODYNAMIC MODEL FOR THE SMELTER GASIFIER AND THE REDUCTION SHAFT

The COREX process was developed to produce hot metal by using noncoking fuel as a reductant. In the COREX process, reduction of iron-ore and later its melting takes place in two separate reactors, the reduction shaft and the smelter gasifier, respectively. In reduction shaft, iron oxide is reduced partially to directly reduced iron (DRI) by the countercurrent flow of reduction gas generated in the smelter gasifier. The DRI is discharged directly into the smelter gasifier for further reduction and melting using the gas generated by combustion of noncoking coal and pure oxygen. The top gas from reduction shaft and excess reduction gas are mixed to produce export gas. Liquid iron, slag, and high calorific value export gas are final products. Figures 1 and 2 depict the flow of various input and output stream flows in the smelter gasifier and the reduction shaft, respectively.

For a detailed exergy analysis, there is a need for a composite model of the COREX process (*i.e.*, consisting of separate smelter gasifier and reduction shaft models interlinked through streams) that predicts output of different stream composition at various operating conditions. Lee *et al.*[7] developed a computational model of the smelter gasifier that focused mainly on coal pyrolysis in three zones to predict the composition and temperature of the reducing gas produced in the smelter gasifier. Pal and Lahiri[8] proposed a steady-state model based on the conservation of mass, momentum and heat. This model could accurately predict the composition and temperature of reducing gas only but not the composition of hot metal and slag. Similarly for reduction shaft, a mathematical model has been proposed by Wu *et al.*[9] using mass, momentum, and heat balances in the reduction shaft to examine the temperature and composition of gas and solid phases across the length of the furnace. However, this model does not depict the effect of change in the amount and composition of reducing gas on the composition of DRI. Srivastava *et al.*[10] proposed a thermodynamic model of the smelter gasifier for predicting the composition of the output streams. In the current work, a thermodynamic model for the reduction shaft has been proposed, and it has been coupled to the modified smelter gasifier model for predicting the composition of different output streams. Finally, the stream data (at various operating conditions) obtained from the proposed models were been used to perform an exergy analysis for the COREX process.

The previously published thermodynamic model[10] has been found to predict accurately the volume of reducing gas produced in a smelter gasifier but fails to provide the exact composition of the gas as reported by Lee *et al.*[7] (low CO_2 and H_2O content). Hence, some changes have been incorporated in the model so as to match the actual chemical composition as well as the volume of gas produced in a smelter gasifier. Moreover, in a previous work,[10] all simulations were performed at a constant coke rate for a particular degree of prereduction, but in the current work, the coke rate has also been varied to ascertain its effect on silicon content in the hot metal.

A. *Thermodynamic Model for Smelter Gasifier*

A schematic diagram of the conceived thermodynamic model for a smelter gasifier is presented in Figure 1.

Its two major input streams, *i.e.*, DRI and coal, are introduced separately into the two submodels of the unit. The DRI is fed into the smelting reduction submodel through reactor E, whereas the coal stream is fed to the coal pyrolysis submodel through reactor A for its devolatization and subsequent burning with oxygen in subsequent reactors like B and C. The composition of the various input streams in the smelter gasifier are mentioned in Appendix A.

1. *Coal pyrolysis submodel*

The composition of coal and its constituents (in moles) as fed into reactor A is mentioned in Appendix A.

FactSage 6.2 permits the definition of a private database for fossil fuels like coal, coke, and fuel oils. It allows the definition of gross heating value, as well as pct C, pct H, and pct S of the fuel, but it does not have any provision for incorporating data with respect to O_2 N_2, and ash content in the coal. Hence, a new approach is proposed for feeding coal as a reactant in the simulations. The input data with respect to coal being fed to reactor A [1073 K (800 °C), 3 atm], are considered as elemental C, H_2, N_2, S, and O_2 (from ultimate analysis of coal) as well as the compounds present in the ash (from proximate analysis of coal). The enthalpy of decomposition of coal has been considered separately in the overall enthalpy balance of the model. It is evident from equilibrium simulations that at 773 K (500 °C), all the volatile matter of coal is expelled (proximate analysis is verified through back calculation from the results of simulations), whereas a higher dome temperature in the gasifier favors the endothermic decomposition of methane. Hence, some volatile carbon in the form of methane and carbon monoxide joins the solid phase (as char) from which lesser volatile carbon is obtained in the gaseous phase in the simulations of reactor A.

The reactor B (at 1503 K [1230 °C], 3 atm) deals with the burning of coal dust and injected secondary O_2, and its amount is assumed in the simulations as 5 pct of the fixed carbon of the coal fed.

The reactor C (at 3 atm) deals with the adiabatic combustion of the char obtained from rector B, and as such, its temperature is the adiabatic flame temperature achieved through the combustion process.

2. *Smelting reduction submodel*

Reactors D and E are placed sequentially to simulate the countercurrent flow of the solids and gases. The
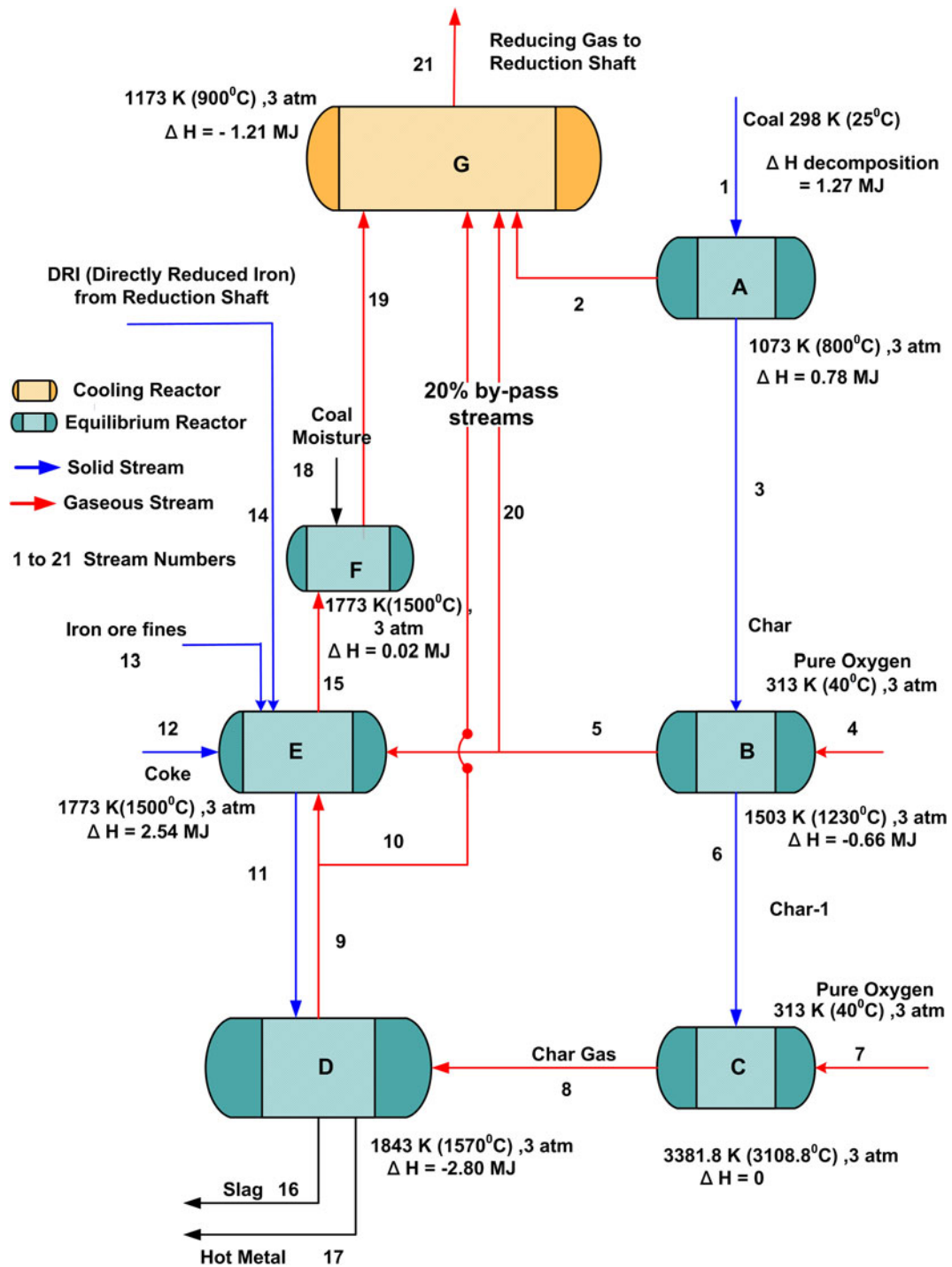
Fig. 1—Thermodynamic model for the smelter gasifier (with 70 pct prereduced DRI input).

reactor D (at 3 atm) receives char gas from the reactor C and the partially formed hot-metal and slag from reactor E, where the streams are equilibrated to produce hot-metal and slag phases of optimum composition as well as the CO-rich gas stream. The temperature of the reactor D is variable (in the range of 1793 K to 1903 K [1520 °C to 1630 °C]) because a low degree of metallization of DRI would demand more coal in the smelter gasifier and thereby lead to an increase in the temperature of the reactor. Hence, the temperature of reactor

D has been varied with the degree of prereduction of DRI to achieve heat balance. In the simulation process, the temperature of the reactor D has been tuned so that the net enthalpy change of all the reactors and the enthalpy of coal decomposition is zero, i.e., $\Sigma\,(\Delta H_{reactors}) + H_{coal\ decomposition} = 0$.

Reactor E (at 1773 K [1500 °C], 3 atm) receives DRI (produced in the reduction shaft), iron ore fines, coke, and the gas streams from the reactors B and D (20 pct of which are considered to by-pass taking into account the
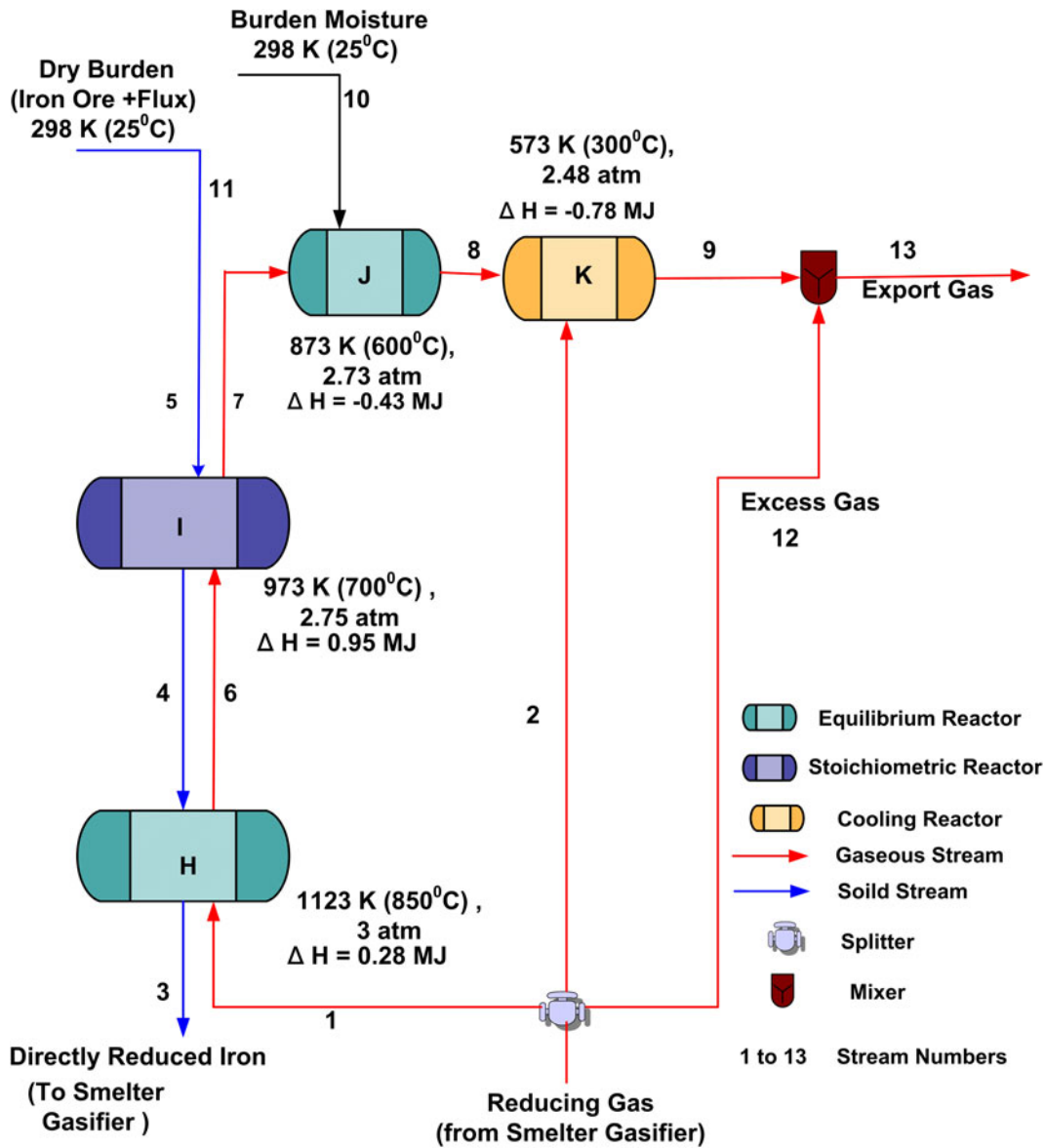
Fig. 2—Thermodynamic model for the reduction shaft (producing 70 pct prereduced DRI).

inefficiency of contact between the solid and gas phases). In this reactor, the total reduction of DRI and its partial melting take place.

Furthermore, the exit gas stream from reactor E has been equilibrated with the coal moisture in reactor F (at 1773 K [1500 °C], 3 atm). The stoichiometric reactions occurring in the different reactors under equilibrium conditions in the smelter gasifier as obtained from FactSage simulations are presented in Appendix B.

The exit gas stream from reactor F is allowed to cool inside reactor G (where no chemical reactions occur) to 1173 K (900 °C) (using the "Reaction Module" of FactSage) by the 20 pct bypassed gas streams from reactors B and D as well as the gas stream from reactor A.

B. Thermodynamic Model for Reduction Shaft

The chemical analysis of the iron bearing ore fed to the reduction shaft is presented in Appendix A.

For the reduction shaft, four reactors have been considered as a part of its thermodynamic model as shown in Figure 2. Reactor H (at 1123 K [850 °C], 3 atm) and reactor I [at 973 K (700 °C), 2.75 atm] are arranged sequentially to simulate the countercurrent flow of solids and gases. It is conceived that reactor I receives a fresh burden, i.e., iron ore and flux, from the top and reducing gas from reactor H in a countercurrent flow system allowing the preheating and partial indirect reduction of the burden (conversion of hematite to wustite). Similarly, reactor H allows a countercurrent flow between the solid coming from reactor I and the reducing gas generated in the smelter gasifier. The output gas stream from reactor I in turn reacts with the moisture from the burden in reactor J (at 873 K [600 °C], 2.73 atm).

Reactor K (at 2.48 atm) cools the output gas stream coming from reactor J and the bypass reducing gas

stream to 573 K (300 °C). A bypass of ~30 pct is assumed to be introduced within the reduction shaft for the reducing gas stream to take into account the inefficiency of contact between the solid and gas phases in the reduction shaft. The exact temperature of exit gas in the range of 523 K to 623 K (250 °C to 350 °C) is determined finally through enthalpy balance; *i.e.*, $\Sigma (\Delta H_{reactors}) = 0$. The stoichiometric reactions occurring in the different reactors of the reduction shaft under equilibrium conditions as obtained from FactSage simulations are presented in Appendix B.

C. Validation of Smelter Gasifier and Reduction Shaft Models

1. Smelter gasifier

The reducing gas composition as well as silicon content of hot metal, obtained from the simulations for the smelter gasifier operating at various degrees of prereductions, match closely the values reported in the literature[7,11] and are presented in Table I and Figures 3 and 4, respectively.

2. Reduction shaft

The average gas use efficiencies for CO, H_2, and both CO and H_2 as obtained from the model simulations are found to be 51 pct, 36 pct, and 47.87 pct, respectively, which are close to the values reported by Wu *et al.*[9] as presented in Table II.

The reducing gas requirements in the reduction shaft and the amount of gas produced in the smelter gasifier while being operated at various degrees of prereductions are shown in Figure 5. It is observed that at higher degrees of prereduction, less excess reducing gas is generated, whereas at 92 pct prereduction, the gas generation in the smelter gasifier is equal to the requirements in the reduction shaft. A similar plot is reported in the literature,[12] where the effective calorific value of coal and energy consumption in smelting and reduction have been considered. Although the predicted volume of gas generated in a smelter gasifier at various degrees of prereduction of DRI, as predicted by the model, has been found to be nearly the same as that reported in literature,[12] the predicted volume of gas requirement according to the currently considered model of the reduction shaft is slightly higher but nonetheless shows a similar trend with the variation of degree of prereduction of DRI.

D. Prediction of Gas Generation in Smelter Gasifier at Varying Coal Rates

To determine the effect of variation of coal rate on the gas generation in the smelter gasifier, simulations have been carried out maintaining the degree of prereduction as constant while varying the coal rates (10 pct less and 10 pct more than the base coal rate) for each degree of prereduction.

It is observed in Figure 6 that the amount of gas generated inside the smelter gasifier follows a linear variation with coal rate irrespective of the degree of prereduction.

III. EXERGY CALCULATION

The exergy (B) of a system or resource is the maximum amount of useful work that can be harnessed from the system when it is brought to equilibrium with the surroundings through reversible processes in which the system is allowed to interact only with the environment.[13]

Table I. Comparison of Simulated Reducing Gas Composition and Literature Data[7]

Composition (vol pct)	CO	H_2	CO_2	H_2O	N_2	CH_4
Simulated	70.49	22.67	2.72	1.14	0.85	2.13
Literature[7]	72.99	18.64	5.10	2.49	0.78	0.01

Fig. 3—Effect of coke rate on Si content in hot metal.

Fig. 4—Variation of Si content in hot metal at various degrees of prereduction.

Table II. Comparison of Simulated Top Gas Use Rates with Literature Data[9]

	CO	H_2	Use Efficiency for Both CO and H_2
Simulated values	51	36	47.87
Literature[9]	45.9	40.5	44.50
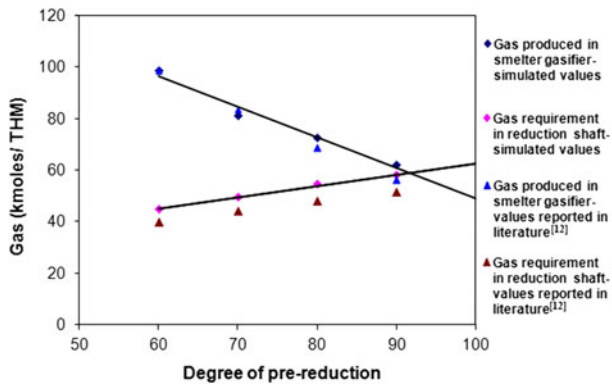
Fig. 5—Reducing gas requirement in the reduction shaft and gas production in the smelter gasifier.

Fig. 7—Schematic representation of exergy losses in process and streams.

Fig. 6—Variation smelter gasifier gas with coal rate.

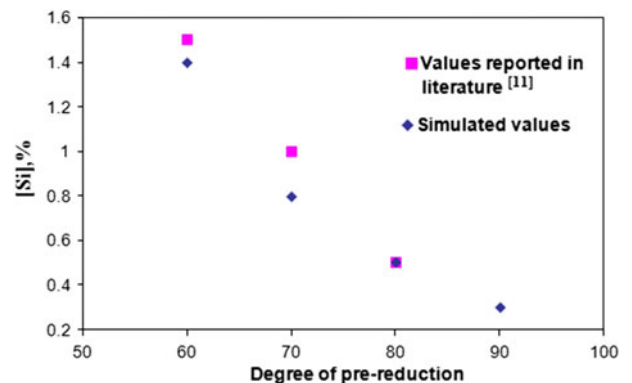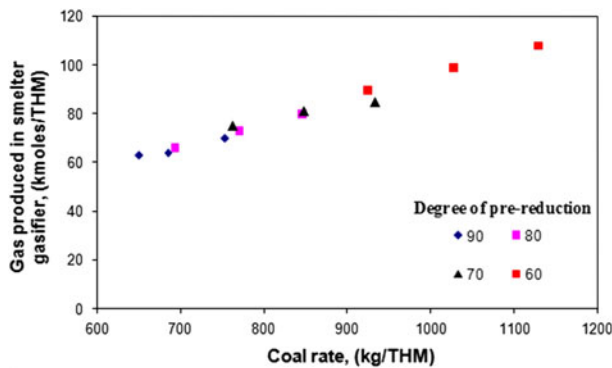Unlike energy, exergy does not follow the law of conservation. In a practical situation, the input and output exergy of a system are not equal, whereas the concept of exergy loss consists of conversion process internal losses as well as undesirable products for solid, liquid, and gas as shown in Figure 7. The desirable products need not be a single stream; they might be certain off gas streams from which it is possible to recover additional exergy.

The exergy loss from the conversion process internal losses ΔB is given by the Gouy–Stodola relation as

$$\Delta B = T_0 \Delta S \qquad [1]$$

Equation [1] points out that the exergy consumption is proportional to entropy generation or it can be stated that the exergy consumption by a process is indicative of its degree of thermodynamic irreversibility.[14]

In the current analysis, the reference compound model as suggested by Szargut et al.[15] has been used. The molar exergy of the pure reference compound can be calculated (as the partial energy released or work performed during an ideal mixing operation that dilutes the pure compound to its reference concentration) from the following equation:

Table III. Comparison of Calculated Mineral Exergy Values with Literature Data[16]

Mineral Name	Chemical Composition	Exergy (kJ/mole)	Exergy (kJ/g)	Literature[16] value (kJ/g)
Galena	PbS	762.14	3.18	3.11
Covellite	CuS	693.13	7.22	7.221
Sphalerite	ZnS	753.85	7.77	7.67
Quartz	SiO$_2$	2.33	0.038	0.032
Aragonite	CaCO$_3$	18.22	0.018	0.01
Boehemite	Al$_2$O$_3$(H$_2$O)	194.7	1.623	1.607
Pyrite	FeS$_2$	1469.24	12.2	11.9

$$B_{\mathrm{mix}} = R.T_0 \sum y_i . \ln\left(\frac{y_i}{y_{0,i}}\right) \qquad [2]$$

where y_i is the moles of component i.

Finally, the standard molar exergy B_j^{ref} for a pure chemical element can be calculated with the formation energy ΔG_f of the corresponding reference compound.

To verify the validity of the FactSage Database, the specific chemical exergies of certain reference and nonreference species have been estimated using Eq. [4] compared with the literature values and presented in Table III.

A. *General Methodology for Estimation of Exergy*

The total exergy of a stream can be estimated as the algebraic sum of chemical exergy and physical exergy of a stream following the methodology described next.

(a) Chemical Exergy (B_{ch}): The estimation of the chemical exergy involves two components like elementary exergy and the free energy of formation of the stream.

    (i) The elementary exergy of the stream has been calculated as a sum of the standard chemical exergies of the elements present in the stream (either in combined or free state) according to

$$B_{el} = \sum_j n_j B_j^{ref} \qquad [3]$$

where B_{el} is the elementary exergy of the stream, B_j^{ref} is the standard chemical exergy of the pure chemical element j at reference conditions, and n_j is the total number of moles of element j present in the stream.

The standard chemical exergy of an element has been taken from the data reported by Szargut.[17]

(ii) Then, the exact same phase(s) as present in the stream has been allowed to be formed from its constituent elements at reference conditions (P_0, T_0) using "Equilibrium Module" of the FactSage 6.2, thus allowing the estimation of the free energy of formation ΔG_f, where ΔG_f represents the work done in producing the phase from its constituent elements. In other words, it can also be considered as the difference in exergy values of the elements present in the phase and the actual phase at reference conditions. Because the actual phase is not stable at reference conditions (T_0 and P_0), i.e., $\Delta G_f > 0$ (if only the phase is allowed to be formed by imposing compositional restrictions), in FactSage simulations, the precursor compounds of the phase are formed by default if no compositional restrictions are imposed.

Accordingly, the chemical exergy of a stream is given by the following relation:

$$B_{ch} = \Delta G_f + B_{el} \qquad [4]$$

(b) Physical Exergy (B_{ph}): The physical exergy of the phase(s) present in a stream is estimated as the work done on the system to take the phase (precursor compounds) from reference conditions (T_0 and P_0) to process conditions (T and P) for the formation of the actual phase(s). This involves the calculation of enthalpy (H) and entropy (S) values with the help of "Equilibrium Module" of FactSage, for the following:

(i) The pre-cursor compounds of the phase at the reference condition (T_0 and P_0)
(ii) The phase at stream condition (T and P).

Accordingly, the physical exergy of a stream has been estimated using the following equation:

$$B_{ph} = (H - H_0) - T_0(S - S_0) \qquad [5]$$

Thus the total exergy of a stream is given by:

$$B_{total} = B_{ch} + B_{ph} \qquad [6]$$

The exergy of streams like slag and hot metal have been calculated following the preceding procedure, which is referred to as the phase based approach.

B. Modifications in Exergy Estimation

1. Gaseous streams

In the calculation of exergy for gaseous streams compound based approach has been adopted.

The chemical exergy of a gas mixture is given by

$$B_{ch} = \sum_i \Delta G_{f,i} + B_{el} + \Delta G_{mix} \qquad [7]$$

where ΔG_f is the free energy of formation of a component i present in the gas mixture.

The free energy of mixing for a gas mixture is given by

$$\Delta G_{mix} = -RT_0 N \sum_i x_i \ln x_i \qquad [8]$$

where x_i is the mole fraction of a component gas in the gas mixture and N is the total moles of gas mixture.

The enthalpy and entropy changes for the change in state from reference conditions (T_0 and P_0) to stream conditions (T and P) has been estimated by the "Reaction Module" of FactSage, which has led to the estimation of physical exergy by using Eq. [5].

2. Solid streams like DRI and iron ore

The exergy of solid streams like iron ore and DRI have also been calculated through a compound-based approach following the same method as adopted for gas stream except that the free energy of mixing ΔG_{mix} for solids has been assumed to be zero.

3. Fuels such as coal and coke

It is not possible to evaluate the exergy of coal and coke directly because they are complex organic substances, and accordingly, their exergy values have been evaluated in the following way:

The specific heating value ($H.V$) of coal, as well as the $\beta = b_{ch}/H.V$ ($=1.078$) corresponding to the approximate chemical composition of the coal have been selected from literature,[18] where b_{ch} is the specific chemical exergy of coal.

Now, using the heating value of coal from literature,[19] its exergy has been found to be 33 MJ/kg. Coke contains 80 pct carbon and so the exergy of coal has been calculated as the equivalent chemical exergy of carbon and the exergy of ash constituents of coke.

C. Validation of Exergy Calculation Methodology for Process Streams

The exergy calculation methodology as discussed applied to the slag of the lead blast furnace, which was analyzed by Szargut et al.[15] In his estimation, the process stream was considered to leave the furnace at 1473 K (1200 °C) with a weight-based slag composition of 39.02 pct FeO, 22.79 pct SiO_2, 16.83 pct ZnO, 13.36 pct CaO, 4.44 pct Pb, 3.23 pct CaS, and 0.34 pct CuO. The estimated values of the current exercise are 2101.67 kJ/kg following the phase-based approach and 1997.35 kJ/kg following the compound-based approach, which compare well with the data of 2035.0 kJ/kg as reported by Szargut et al. It has been observed in the simulation that when all the possible phases are allowed to form at 1473 K (1200 °C), some additional phases like liquid lead ~4 pct and monoxide phase ~2 pct are also formed along with the slag phase, and hence, their exergy have been calculated separately following the phase-based approach as discussed.

IV. EXERGY ANALYSIS OF THE COREX PROCESS

Simulations have been performed for the COREX process operating at 60 pct, 70 pct, 80 pct, and 90 pct prereductions through FactSage 6.2, using the separately conceived thermodynamic models for the smelter gasifier and the reduction shaft. The raw material input[1] used in simulations for 70 pct degree of prereduction of DRI is presented in Table IV. The values reported in the table correspond to average input data.

The resulting data for various output streams (like composition, temperature, and pressure) was used to perform an exergy analysis using the previously mentioned methodology. The pertaining results for 70 pct pre-reduction corresponding to the smelter gasifier and the reduction shaft are presented in Tables V and VI, respectively.

Various authors have reported different values of exergy loss for blast furnace. Ostrovski et al.[5] have found an exergy loss of 5461 MJ/THM (while considering blast furnace and blast stove), but there is no mention of the composition and amount of the input and output streams. Nogami et al.[6] reported an exergy loss value of 4290 MJ/THM (while considering exergy losses in coke making, sintering, blast furnace, and blast stove) and mentioned the composition of input streams only. However, the chosen criteria for calculation of exergy values of input and output streams in both these reports are not mentioned clearly.

The exergy flow for the COREX process operating at 70 pct prereduction is presented by a Sankey-Grassmann Diagram in Figure 8.

Similar calculations have been performed for the COREX process operating at 60, 80, and 90 pct prereductions at the different base coal rates as mentioned in Table VII, and the corresponding data are presented in Figure 9. This figure demonstrates clearly that the exergy loss increases linearly with the input coal rate. While comparing literature values, it is found that the exergy destroyed in blast furnace[6] (equivalent coal rate 620 kg/THM) is slightly lower than that in a COREX process (operating at coal rate of 685 kg/THM). This leads to the conclusion that irreversibility associated with combustion of coal/coke is a major source of exergy loss in iron-making processes.

A. Exergy Efficiencies

The efficiency of a process is an important yardstick for deciding its economic value in terms of resource consumption, which paves way for an effective comparison of industrial processes producing similar products.

Efficiency is defined as the ability to produce a desired effect without any wastage or with minimum use of energy, time, resources, etc.[14] Exergy efficiency predicts accurately the effectiveness of a process because it incorporates the limitations imposed on the process by the second law of thermodynamics, unlike energy efficiency, which is only partially accurate. The exergy efficiency is defined as the ratio of the final product exergy (or useful effect of a process) to the total exergy of resources consumed, including all the exergy inputs. In the case of iron-making processes, two types of exergy efficiencies can be considered depending on the type of outputs as valuable products. In the current study, two efficiencies are discovered, namely

(1) hot-metal based efficiency (Ψ_m), when only hot metal is the useful product

Table V. Exergy Balance for Smelter Gasifier for 70 Pct Prereduction

Stream	Mass Flow (kg)	Temperature [K (°C)]	Exergy (MJ)
(a) Inflow			
Coal	850	298 (25)	28,050
Coke	150	298 (25)	4102.6
DRI (70pct)	1150	1073 (800)	5288.06
Fines	100	298 (25)	17.93
O₂ gas	544.32 (m³)	313 (40)	204.68
Total			37,663.28
(b) Outflow			
Hot metal	1000	1843 (1570)	8927.60
Slag	342.5	1843 (1570)	887.42
Reduction gas	1818.18 (m³)	1173 (900)	22907.65
Total			32722.67

Therefore, exergy loss in the smelter gasifier
= (exergy inflow) − (exergy outflow).
= (37663.28) − (32722.67).
= **4940.61** MJ/THM.

Table VI. Exergy Balance for Reduction Shaft Producing 70 Pct DRI

Stream	Mass Flow (kg)	Temperature [K (°C)]	Exergy (MJ)
(a) Inflow			
Ore + Flux	1597	298 (25)	287.61
Reduction gas (from smelter gasifier)	1136 (m³)	1173 (900)	14,316
Total			14,603.61
(b) Outflow			
Off gas	1145 (m³)	573 (300)	8683
DRI (70 pct)	1150	1073 (800)	5288.06
Total			13971.06

Therefore, the exergy loss in the reduction-shaft is as follows:
= (exergy inflow) − (exergy outflow).
= (14,603.61) − (13,971.06).
= **632.55** MJ/THM.
Hence, total exergy destroyed in the COREX process = 4940.61 + 632.55 = **5573.16** MJ/THM.

Table IV. Raw Material Input Used in Simulation of the COREX Process Operating at 70 Pct Prereduction

Inputs	Amount
Iron ore pellets	1340 kg/THM
Iron ore fines	100 kg /THM
Flux	257 kg/THM
Coal	850 kg/THM
Coke	150 kg/THM
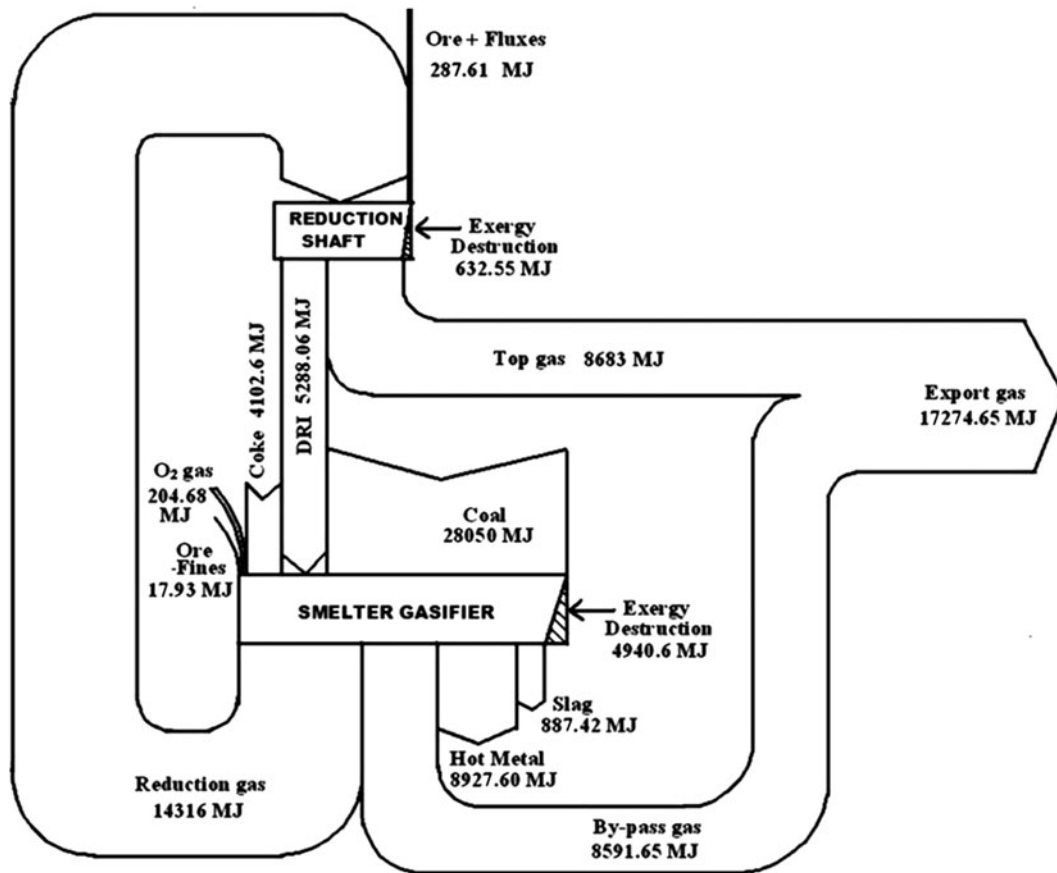
Fig. 8—Sankey-Grassmann diagram for the COREX process operating at 70 pct prereduction.

Table VII. Base Coal Rates for Different Degrees of Prereduction

Degree of Prereduction	Base Coal Rate (kg/THM)	Coke Rate (kg/THM)
60	1028	173
70	850	150
80	770	127.5
90	685	105

$$\Psi_m = B_{metal}/B_{input} \qquad [9]$$

(2) hot-metal + gas-based efficiency ($\Psi_{g\text{-}m}$), when hot metal as well as the export gas are the useful products

$$\Psi_{g-m} = (B_{metal} + B_{export-gas})/B_{input} \qquad [10]$$

The estimated exergy efficiency of the COREX process operating at various degrees of prereductions as a function of coal rate have been compared with that of the blast furnace and presented in Figure 10. The coal rate presented in this figure for blast furnace is an equivalent coal rate, *i.e.*, the actual coal rate required to produce coke to be used in the blast furnace. Also, the input exergy values of the ores have been assumed to be the same for both the blast furnace as well as the
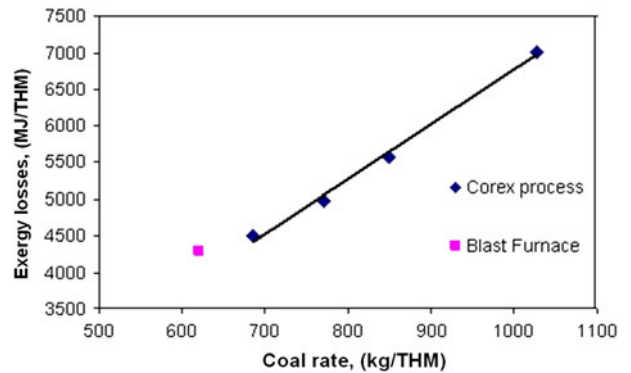
Fig. 9—Exergy lost at various degrees of prereduction at base coal rates.

COREX process. The $\Psi_{g\text{-}m}$ values of the blast furnace have been calculated by taking into account the exergy values[6] of the blast furnace top gas, coke oven gas, and other useful products of the process.

It is found that $\Psi_{g\text{-}m}$ (*i.e.*, metal + gas)-based efficiencies of the COREX process are nearly the same for various coal rates and marginally higher than that of the blast furnace. In the COREX process, with an increase in the degree of prereduction (*i.e.*, decrease in the coal rate), the hot-metal based efficiency (*i.e.*, Ψ_m) increases. At lower coal rates, hot-metal–based efficiencies of the COREX process are slightly lower than blast furnace.
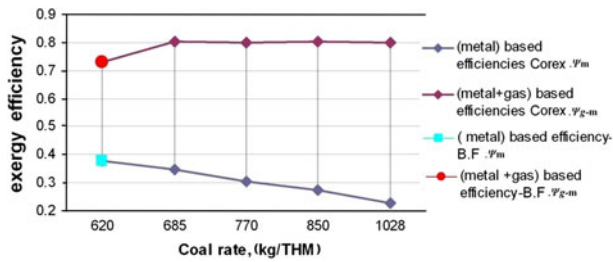
Fig. 10—Exergy efficiencies of the COREX process and blast furnace.

Thus, if power generation from export gas is not economical, then to produce the same amount of valuable product (hot metal), higher exergy loss results if the COREX process is operated at higher coal rates. So it is preferable to operate the COREX process at lower coal rates if power generation is not feasible.

V. SUMMARY AND CONCLUSIONS

A composite thermodynamic model (*i.e.*, models for the smelter gasifier and the reduction shaft) of the COREX process has been developed in obtaining process stream information for exergy calculations. The model has been validated by comparing output stream compositions and quantities with literature data (smelter and shaft gas compositions, reduction gas requirements of shaft) and has been found to be in good agreement with the published values. This model has been used for obtaining exergy values of process streams at various operating coal rates.

A methodology for calculating exergy of process streams using the Factsage database has been developed. The methodology has been validated against published exergy values of streams of known compositions. An exergy analysis of the COREX process performed at various input coal rates (685 to 1028 kg/THM) leads to the following observations:

1. Exergy loss (4500 to 7015 MJ/THM) is found to vary linearly with the coal rate, thus providing support to the idea that the combustion of carbon is a major source of irreversibility in the COREX process.
2. Exergy efficiencies evaluated at various coal rates (considering hot-metal/hot metal and export gas as useful products) show that the efficiency of the CO-REX process (hot metal basis) varies from 22 pct to 34 pct, and a decrease in coal rate results in an increase in efficiency. However, when both hot-metal and export gas are considered as useful products, the efficiency is nearly constant (approximately 80 pct) at various coal rates.

3. Literature data have been used for computing blast furnace exergy efficiency (620 kg/THM coal rate to coke ovens). The efficiency on a hot metal basis (37.65 pct) has been found to be generally higher than that of the COREX process at various coal rates. Thus, the blast furnace process seems to be more sustainable if only hot metal is the useful product. However, the blast furnace efficiency considering both hot metal and export gas as useful products (73 pct) is lower than the COREX process efficiency (80 pct). This is because of the low calorific value of the top gas and also because of the relatively low volume of coke oven gas that is generated.
4. In situations when power generation from export gas is not economical, it is preferable to operate the COREX process at lower coal rates (650 to 700 kg/THM) so that the heat requirement is satisfied in the smelter gasifier and enough reducing gas is generated to produce DRI in the reduction shaft.

APPENDIX A

Coal Composition

Table A1. Ultimate Analysis of Coal (On Dry Mineral Matter Free Basis)

C (wt pct)	H (wt pct)	N (wt pct)	O (wt pct)	S (wt pct)
86.52	5.27	2.37	5.20	0.64

Table A2. Proximate Analysis

Fixed Carbon (wt pct)	Volatile Matter (wt pct)	Ash (wt pct)	Moisture (wt pct)
58	27	10	5

Table A3. Ash Analysis of Coal

Constituent	SiO_2	Al_2O_3	FeO	CaO	MgO	P_2O_5	TiO_2	SO_3
Wt pct	58	31	3.58	2.72	1.33	0.669	0.70	0.908

Table A4. Molar Composition of Coal Feed Used in Simulations, Kmoles (Base Coal Rate of 850 kg/THM for the COREX Process Operating at 70 pct Prereduction)

Constituent quantity	C	SiO_2	Al_2O_3	TiO_2	MgO	CaO	P_2O_5
kmoles	55.07	0.821	0.258	0.0074	0.028	0.0412	0.004

Constituent quantity	SO_3	FeO	H_2	N_2	O_2	S
kmoles	0.0096	0.042	20.15	0.647	1.24	0.153

Table A5. Proximate Analysis of Coke

Fixed Carbon (wt pct)	Volatile Matter (wt pct)	Ash (wt pct)	Moisture (wt pct)
80	1	13	6

Table A6. Ash Analysis of Coke

Constituent	SiO_2	Al_2O_3
Wt pct	58	31

Table A7. Molar Composition of Ore Fines Feed Used in the Simulations (kmoles)

Constituent	Fe_2O_3	SiO_2	Al_2O_3	CaO	P
kmoles	0.575	0.058	0.024	0.033	0.00193

Table A8. Iron Ore Composition

Fe (wt pct)	SiO_2 (wt pct)	Al_2O_3 (wt pct)	CaO (wt pct)	Basicity (CaO/SiO_2)
63.5	3.5	2.5	1.86	0.53

Table A9. Molar Composition of Iron Ore Feed Used in Simulations (kmoles)

Constituent	Fe_2O_3	SiO_2	Al_2O_3	CaO	$CaCO_3$	MgO	$MgCO_3$	MnO_2	P
kmoles	7.7	1.02	0.3180	0.44	1.67	0.21	0.8	0.018	0.025

Iron Ore Composition

For 70 pct prereduction, the various constituents of iron-ore fines fed to the smelter gasifier and their molar quantities fed in the simulations are given in Tables A7 through A9.

For 70 pct prereduction, the various constituents of iron ore and fluxes fed to reduction shaft, and their molar quantities fed in simulation are given in Table A9.

APPENDIX B

Reactions in Smelter Gasifier

The stoichiometric reaction (on molar basis) occurring in various reactors of the smelter gasifier model obtained from FactSage simulation is given by

Reactor A

$$(55.07C + 40.3H + 1.294N + 2.48O + 0.153S)_{coal}$$
$$+ (0.821SiO_2 + 0.258Al_2O_3 + 0.0074TiO_2$$
$$+ 0.028MgO + 0.0412CaO + 0.004P_2O_5$$
$$+ 0.0096SO_3 + 0.042FeO)_{Ash}$$
$$\rightarrow (55.07C + 0.821SiO_2 + 0.258Al_2O_3$$
$$+ 0.0074TiO_2 + 0.028MgO + 0.0412CaO$$
$$+ 0.004P_2O_5 + 0.0096SO_3 + 0.042FeO$$
$$+ 0.153S)_{(s)\,char} + (20.15H_2 + 0.647N_2$$
$$+ 1.24O_2)_{(g)} \qquad [B1]$$

$$(55.07C + 0.821SiO_2 + 0.258Al_2O_3 + 0.0074TiO_2$$
$$+ 0.028MgO + 0.0412CaO + 0.004P_2O_5$$
$$+ 0.0096SO_3 + 0.042FeO + 0.153S)_{(s)\,char}$$
$$+ (20.15H_2 + 0.647N_2 + 1.24O_2)_{(g)}$$
$$\rightarrow (16.1H_2 + 1.82CO + 1.73CH_4$$
$$+ 0.647N_2 + 0.554H_2O + 0.0686CO_2)_{(g)}$$
$$+ (51.5C + 0.821SiO_2 + 0.258Al_2O_3 + 0.163S$$
$$+ 0.0420FeO + 0.0412CaO + 0.028MgO$$
$$+ 0.0074TiO_2 + 0.004P_2O_5)_{(s)\,char} \qquad [B2]$$

Reactor B

$$6.25O_{2(g)} + (51.5C + 0.821SiO_2 + 0.258Al_2O_3$$
$$+ 0.163S + 0.0420FeO + 0.0412CaO$$
$$+ 0.028\,MgO + 0.0074TiO_2 + 0.004P_2O5)_{(s)\,Char}$$
$$\rightarrow (12.51CO + 0.02CO_2)_{(g)} + (38.97C$$
$$+ 0.821SiO_2 + 0.258Al_2O_3 + 0.163S + 0.042FeO$$
$$+ 0.0412CaO + 0.028MgO + 0.0074TiO_2$$
$$+ 0.004P_2O5)_{(s)\,Char} \qquad [B3]$$

Reactor C

$$19.08O_2 + (38.97C + 0.821SiO_2 + 0.258Al_2O_3$$
$$+ 0.163S + 0.042FeO + 0.0412CaO$$
$$+ 0.028MgO + 0.0074TiO_2 + 0.004P_2O_5)_{(s)\,char,}$$
$$\rightarrow (38.97CO + 0.821SiO + 0.163S$$
$$+ 0.042FeO + 0.0412CaO + 0.028MgO$$
$$+ 0.0074O_2Ti + 0.004O_5P_2)_{(Char\,gas)}$$
$$+ 0.258Al_2O_3\,(liq) \qquad [B4]$$

Reactor D

$$(38.97CO + 0.821SiO + 0.163S + 0.042FeO$$
$$+ 0.0412CaO + 0.028MgO + 0.0074TiO_2$$
$$+ 0.004O_5P_2)_{(g)} + 0.258Al_2O_3\,(liq) + 0.198SiO_2$$
$$+ 0.231MgO\,(s) + (0.778MgO + 1.077SiO_2$$
$$+ 2.142CaO + 0.350Al_2O_3 + 0.001FeO)_{slag}$$
$$+ (16.546Fe + 3.1433C + 0.017Mn + 0.026P)_{metal}$$
$$\rightarrow (38.72CO + 0.01CO_2)_{(g)} + (0.987MgO + 0.0014FeO$$
$$+ 0.0021MnO + 1.89SiO_2 + 0.0013TiO_2$$
$$+ 0.0015Ti_2O_3 + 2.07CaO + 0.639Al_2O_3$$
$$0.0495MgS + 0.104CaS)_{slag} + (16.575Fe + 3.389C$$
$$0.014Mn + 0.0349P + 0.0001S + 0.1949Si$$
$$+ 0.0028Ti + 0.0129FeS)_{hot-metal} \qquad [B5]$$

Reactor E

$$10C_{(s)} + (0.575Fe_2O_3 + 0.058SiO_2 + 0.024Al_2O_3$$
$$+ 0.033CaO + 0.00193P)_{(s),\,Fines} + (10.62Fe$$
$$+ 4.24FeO + 0.173MgO + 0.018MnO$$
$$+ 0.269Ca_2Fe_2O_5 + 0.327MgAl_2O_4$$
$$+ 0.51MgOCa_3O_3Si_2O_4$$
$$+ 0.00833Ca_5HO_{13}P_3)_{(s),\,DRI}$$
$$+ (0.013CO_2 + 40.93CO)_{(g)}$$
$$\rightarrow (47.79CO + 0.0278CO_2 + 0.004H_2)_{(g)}$$
$$+ (0.778MgO + 1.077SiO_2 + 2.142CaO$$
$$+ 0.350Al_2O_3 + 0.001FeO)_{slag} + (16.546Fe$$
$$+ 3.1433C + 0.017Mn + 0.026P)_{hot-metal} \qquad [B6]$$

Reactor F

$$(47.79CO + 0.0278CO_2 + 0.004H_2 + 2.35H_2O)_{(g)}$$
$$\rightarrow (45.77CO + 2.047CO_2 + 2.02H_2 + 0.33H_2O)_{(g)} \qquad [B7]$$

Reactions in Reduction Shaft

The stoichiometric reaction (on molar basis) occurring in various reactors of the Reduction Shaft model obtained from FactSage simulation is given by

Overall reaction in the reduction shaft

$$(7.7000Fe_2O_3 + 1.020SiO_2 + 0.3180Al_2O_3 + 0.4400CaO$$
$$+ 1.67CaCO_3 + 0.210MgO + 0.8000MgCO_3\,(s)$$
$$+ 0.0180MnO_2\,(s) + 0.0250P)_{Ore+Flux\,(s)} + H_2O_{(l)}$$
$$+ (35.0497CO + 1.3636CO_2 + 11.1219H_2$$
$$+ 0.5582H_2O + 0.3947N_2 + 1.0555CH_4)_{(g)}$$
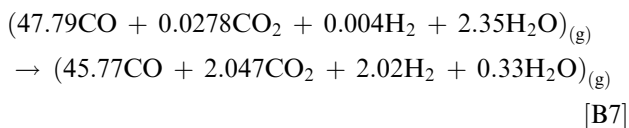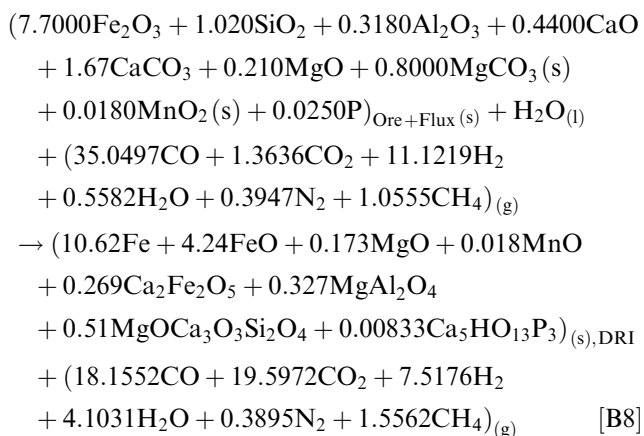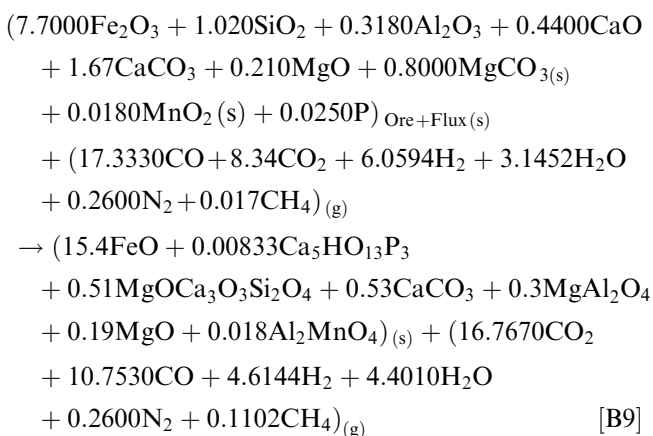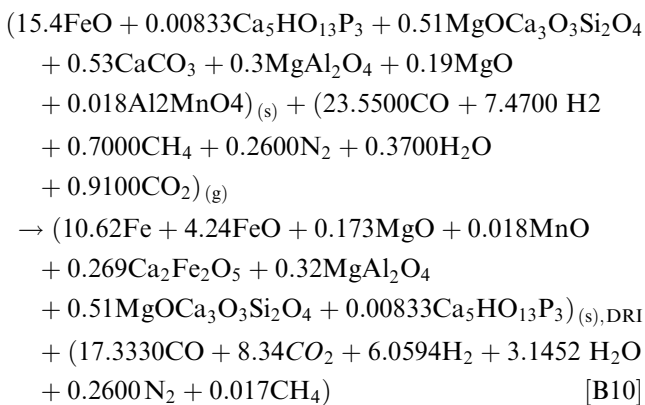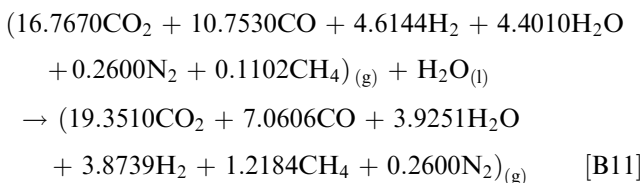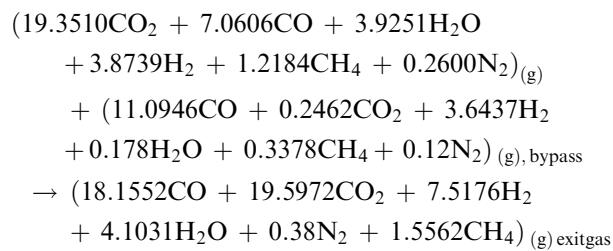$$\rightarrow (10.62Fe + 4.24FeO + 0.173MgO + 0.018MnO$$
$$+ 0.269Ca_2Fe_2O_5 + 0.327MgAl_2O_4$$
$$+ 0.51MgOCa_3O_3Si_2O_4 + 0.00833Ca_5HO_{13}P_3)_{(s),DRI}$$
$$+ (18.1552CO + 19.5972CO_2 + 7.5176H_2$$
$$+ 4.1031H_2O + 0.3895N_2 + 1.5562CH_4)_{(g)} \qquad [B8]$$

Reactor I

$$(7.7000Fe_2O_3 + 1.020SiO_2 + 0.3180Al_2O_3 + 0.4400CaO$$
$$+ 1.67CaCO_3 + 0.210MgO + 0.8000MgCO_{3(s)}$$
$$+ 0.0180MnO_2\,(s) + 0.0250P)_{Ore+Flux\,(s)}$$
$$+ (17.3330CO + 8.34CO_2 + 6.0594H_2 + 3.1452H_2O$$
$$+ 0.2600N_2 + 0.017CH_4)_{(g)}$$
$$\rightarrow (15.4FeO + 0.00833Ca_5HO_{13}P_3$$
$$+ 0.51MgOCa_3O_3Si_2O_4 + 0.53CaCO_3 + 0.3MgAl_2O_4$$
$$+ 0.19MgO + 0.018Al_2MnO_4)_{(s)} + (16.7670CO_2$$
$$+ 10.7530CO + 4.6144H_2 + 4.4010H_2O$$
$$+ 0.2600N_2 + 0.1102CH_4)_{(g)} \qquad [B9]$$

Reactor H

$$(15.4FeO + 0.00833Ca_5HO_{13}P_3 + 0.51MgOCa_3O_3Si_2O_4$$
$$+ 0.53CaCO_3 + 0.3MgAl_2O_4 + 0.19MgO$$
$$+ 0.018Al2MnO4)_{(s)} + (23.5500CO + 7.4700\,H_2$$
$$+ 0.7000CH_4 + 0.2600N_2 + 0.3700H_2O$$
$$+ 0.9100CO_2)_{(g)}$$
$$\rightarrow (10.62Fe + 4.24FeO + 0.173MgO + 0.018MnO$$
$$+ 0.269Ca_2Fe_2O_5 + 0.32MgAl_2O_4$$
$$+ 0.51MgOCa_3O_3Si_2O_4 + 0.00833Ca_5HO_{13}P_3)_{(s),DRI}$$
$$+ (17.3330CO + 8.34CO_2 + 6.0594H_2 + 3.1452\,H_2O$$
$$+ 0.2600\,N_2 + 0.017CH_4) \qquad [B10]$$

Reactor J

$$(16.7670CO_2 + 10.7530CO + 4.6144H_2 + 4.4010H_2O$$
$$+ 0.2600N_2 + 0.1102CH_4)_{(g)} + H_2O_{(l)}$$
$$\rightarrow (19.3510CO_2 + 7.0606CO + 3.9251H_2O$$
$$+ 3.8739H_2 + 1.2184CH_4 + 0.2600N_2)_{(g)} \qquad [B11]$$

Reactor K

$$(19.3510CO_2 + 7.0606CO + 3.9251H_2O$$
$$+ 3.8739H_2 + 1.2184CH_4 + 0.2600N_2)_{(g)}$$
$$+ (11.0946CO + 0.2462CO_2 + 3.6437H_2$$
$$+ 0.178H_2O + 0.3378CH_4 + 0.12N_2)_{(g),\,bypass}$$
$$\rightarrow (18.1552CO + 19.5972CO_2 + 7.5176H_2$$
$$+ 4.1031H_2O + 0.38N_2 + 1.5562CH_4)_{(g)\,exitgas}$$

[B12]

NOMENCLATURE

DRI	directly reduced iron
THM	tone of hot metal
B, b	exergy (J)
Δ	change of a quantity
G	free energy of formation (J)
H	enthalpy (J)
S	entropy (J/K)
T	temperature (K ($^{\circ}$C))
x	mole fraction
N	total moles of gas mixture
Ψ	exergy efficiency

SUBSCRIPT/SUPERSCRIPT

coal decomposition	property of coal
o	property at reference conditions
ch, ph	property derived from chemical phenomena and physical phenomena, respectively
f	property associated with reaction leading to formation of compound or phase
mix	property associated with mixing phenomenon
el	property derived from elemental composition of a phase

i, j	indices for counting gaseous components and elements present in stream, respectively
ref	at reference conditions
metal, export gas	property associated with hot-metal and export gas, respectively
$m, g\text{-}m$	considering hot metal and hot metal + export gas as valuable product(s), respectively

REFERENCES

1. P.P. Kumar, P.K. Gupta, and M. Ranjan: *Ironmaking Steelmaking*, 2008, vol. 35 (4), pp. 260–63.
2. J. de Beer, E. Worrell, and K. Blok: *Ann. Rev. Energ. Environ*, 1998, vol. 23 (1), pp. 123–205.
3. M.M. Costa, R. Schaeffer, and E. Worrell: *Energy*, 2001, vol. 26 (4), pp. 363–84.
4. R. Petela, W. Hutny, and J.T. Price: *Adv. Environ. Res.*, 2002, vol. 6 (2), pp. 157–70.
5. O. Ostrovski and G. Zhang: *Energy*, 2005, vol. 30 (15), pp. 2772–83.
6. H. Nogami, J. Yagi, and S. Sampaio: *Iron Steel Inst. Jpn. Int.*, 2004, vol. 44 (10), pp. 1646–52.
7. S.C. Lee, M.K. Shin, S. Joo, and J.K. Yoon: *Iron Steel Inst. Jpn. Int.*, 1999, vol. 39 (4), pp. 319–28.
8. S. Pal and A.K. Lahiri: *Metall. Mater. Trans. B*, 2003, vol. 34B, pp. 103–14.
9. S. Wu, J. Xu, S. Yang, Q. Zhou, and L. Zhang: *Iron Steel Inst Jpn. Int.*, 2010, vol. 50 (7), pp. 1032–39.
10. B. Srivastava, S.K. Roy, and P.K. Sen: *Metall. Mater. Trans. B*, 2010, vol. 41B, pp. 935–39.
11. P.P. Kumar, P.K. Gupta, and M. Ranjan: *Ironmaking Steelmaking*, 2008, vol. 35 (2), pp. 108–13.
12. P.S. Assis, L. Guo, J. Fang, and T.R. Mankhand: *Ironmaking Steelmaking*, 2008, vol. 35 (4), pp. 303–07.
13. J. Dewulf, H.V. Lagenhove, B. Muys, S. Bruers, B. Bakshi, G.F. Grubb, D.M. Paulus, and E. Sciubba: *Environ. Sci. Tech.*, 2008, vol. 42 (7), pp. 2221–32.
14. I. Dincer and M.A. Rosen: *Exergy: Energy, Environment and Sustainable Development*, 1st ed., Elsevier, Burlington, MA, 2007, pp. 1–22.
15. J. Szargut, D.R. Morris, and F.R. Steward: *Exergy Analysis of Thermal, Chemical and Metallurgical Processes*, Hemisphere Publishing Company, New York, NY, 1988.
16. G. Finnveden and P. Ostlund: *Energy*, 1997, vol. 22 (9), pp. 923–31.
17. J. Szargut: *Appl. Energ.*, 1989, vol. 32 (4), pp. 269–86.
18. A. Srivastava: *Energ. Convers. Mgmt*, 1988, vol. 28 (2), pp. 117–21.
19. P.P. Kumar and M. Ranjan: STEEL TECH, 2009, *Proc. of International Seminar on Alternative Routes of Iron-Making in India*, Kolkata, India, pp. 29–33.